

# **Chapter Five**

## **PolyTPD-based Photorefractive Polymers**

### **Abstract**

Two novel photorefractive host-guest materials based on a novel charge-transporting polymer are presented. This host polymer consists of the well-known charge transport molecule TPD. The photorefractive polymers exhibit high electro-optic effects, but their gain coefficient and diffraction efficiency are rather small. This is attributed to a rather weak space-charge field, caused by a deficiency of trapping sites. An attempt to increase the amount of trapping sites by incorporating additional trapping molecules is described.

### 5.1. Introduction

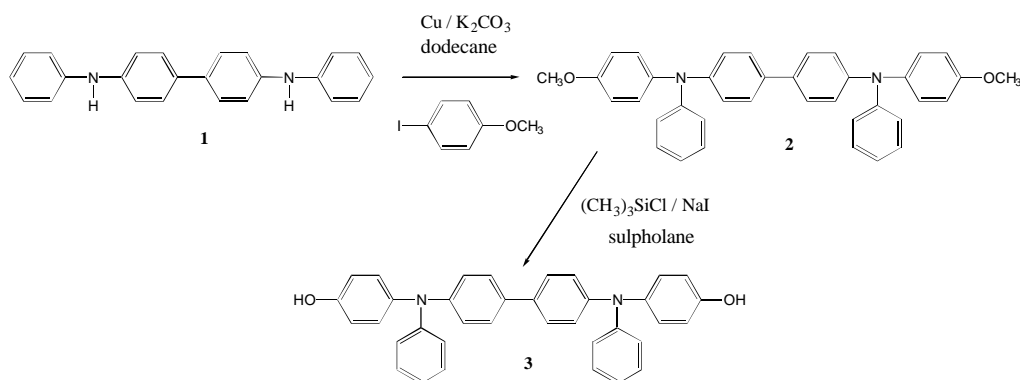
In chapter four a photorefractive composite was described utilizing a bifunctional molecule that was based on the very efficient charge transport molecule TPD<sup>1</sup>. This composite has some attractive properties such as low intrinsic trap density resulting in a phase shift of 90° between the illumination pattern and the refractive index grating. A 90° phase shift is desirable for applications based on optical amplification, as the energy exchange between two beams depends strongly on this phase shift<sup>2</sup>. Furthermore, addition of small amounts of trap molecules allows the tunability of the characteristics of such a polymer. The main disadvantage of this bifunctional molecule based polymer is the relatively low magnitude of the photorefractive effect. This is caused partly by the low space-charge field, but, as was demonstrated for the composite containing large amounts of trapping sites, also by a low effective electro-optic coefficient. In polymers the conversion of the space-charge field to a refractive index grating occurs via both the Pockels and the Kerr effect as was described in chapter one<sup>3</sup>. Both these processes depend on the kind and the amount of electro-optic molecules present and on their orientational freedom. In bifunctional molecules both the charge transport and the electro-optic properties are combined, which limits the tunability of the electro-optic part. Furthermore, the orientational freedom of these electro-optic parts is restricted because they are part of a much larger molecule. We have therefore, taken another approach in the preparation of a photorefractive polymer based on TPD. The class of photorefractive polymers that results in the highest orientational freedom and hence the highest conversion of the space-charge field to a refractive index change are the polymers in which at least the electro-optic molecules are dispersed<sup>4,5</sup>. In order to prevent phase separation of either the NLO or the TPD molecule and still incorporate large amounts of NLO molecules, it is necessary to incorporate TPD in the host polymer. An additional advantage of host-guest photorefractive polymers is the larger tunability, i.e. a wider range of possibilities to change the material properties by choosing different kinds of NLO molecules.

In this chapter we describe the synthesis and the characterization of a photorefractive host-guest polymer composite based on a TPD-containing host-polymer. Two different kinds of photorefractive polymers were prepared and characterized, one using the NLO molecule 4-(*N,N*-diethylamino)nitrobenzene (EPNA), described in chapter three, and another using the very efficient liquid NLO molecule, 4-(*N,N*-diethylamino)-3-fluoro-(*Z*)- $\beta$ -methyl-(*E*)- $\beta$ -nitrostyrene<sup>6</sup> (FDEAM-NST).

## 5.2. Materials

### 5.2.1. Synthesis

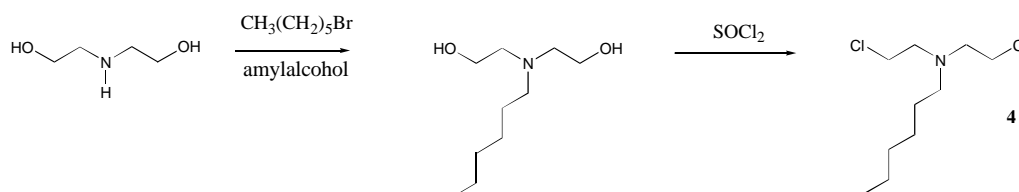
The TPD-containing monomer required for the preparation of a soluble polymer was prepared starting from *N,N'*-diphenylbenzidine **1** (scheme 5.1).



*Scheme 5.1: The synthetic route to obtain the TPD monomer.*

The required bifunctionality was introduced by means of the methoxy groups of 4-iodoanisole which was reacted with **1** in a typical Ullman-like reaction. The resulting dimethoxy-TPD **2** could be converted to the dihydroxy-TPD **3** by treatment with trimethylsilylchloride and sodium iodide. This monomer can then be polymerized in various ways. The preparation of a polyether was chosen over other polymers, such as polyesters or polycarbonates, because polyethers have the most flexible backbone. Polyethers can be prepared in numerous ways, the simplest way is the reaction between a dihydroxy- and a dihalogenalkane compound. A polymerization technique based on a phase transfer polyetherization was used<sup>7</sup>. Using this technique, good yields of polymers, with moderate average molecular weights, were obtained by reacting the dihydroxy-TPD with a number of commercially available linear dihalogenalkanes. These polymers, however, did not give transparent films after solvent casting. The quality of the films did improve with decreasing spacer length, but a completely transparent film could not be obtained. The reason for this behaviour is not completely understood. With smaller alkane spacers, however, less opaque polymer films are obtained, indicating that with increasing aliphatic spacer length more phase separation or crystallization occurs. The relatively long spacers (at least six carbon atoms) that were used are necessary to give soluble polymers. One way to overcome this minimum spacer length restriction is introducing a solubilizing side chain into the monomer unit. Such a monomer, **4** was prepared according to scheme 5.2. Starting from

diethanolamine, a hexyl chain was introduced by nucleophilic substitution, which is followed by chlorination at the hydroxy groups using thionyl chloride.



**Scheme 5.2:** The synthetic route to obtain the hexyl-substituted dichloroalkane monomer.

The polyether based on dihydroxy-TPD and monomer 4, hereafter referred to as polyTPD (the chemical structure is shown in figure 5.1), did indeed give fully transparent films. The weight average molecular weight was 31000 and the number average molecular weight was 16000 as determined with GPC. The  $T_g$  of this polymer was 72 °C.

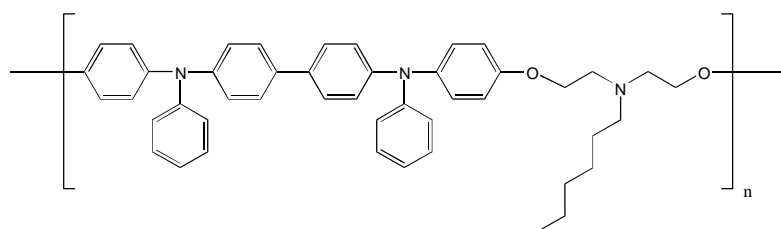
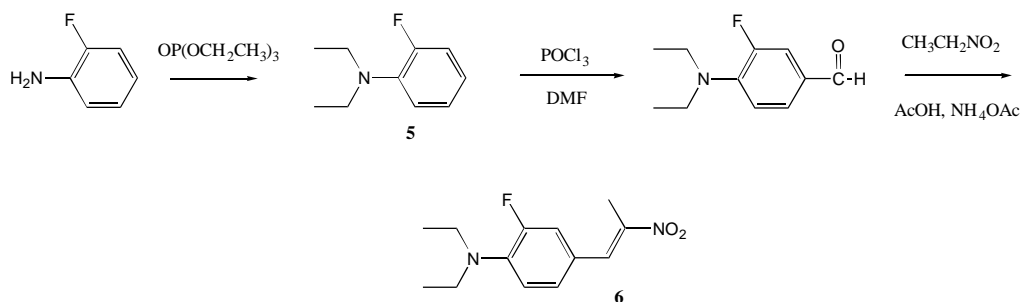


**Fig. 5.1:** Chemical structure of polyTPD.

The synthesis of EPNA was described in chapter three and will therefore not be repeated here. The other NLO molecule, 4-(*N,N*-diethylamino)-3-fluoro-(*Z*)- $\beta$ -methyl-(*E*)- $\beta$ -nitrostyrene<sup>6</sup> (FDEAMNST), was synthesized according to scheme 5.3. 2-Fluoroaniline is ethylated with triethyl phosphate. The compound **5** is then formylated in a Vilsmeier reaction; subsequent condensation with nitroethane gives the desired NLO molecule **6**.

### 5.2.2. Sample preparation

The electro-optic and photorefractive measurements were performed on approximately 100  $\mu\text{m}$  thick polymer films. The films were prepared from toluene solutions containing the proper amount of the necessary compounds.



**Scheme 5.3:** The synthetic route to obtain the electro-optic molecule FDEAMNST.

The EPNA-containing composites consisted of 20 wt.% EPNA, 79.8 wt.% polyTPD and 0.2 wt.%  $\text{C}_{60}$ . The FDEAMNST-containing composite consisted of 30 wt.% FDEAMNST, 69.8 wt.% polyTPD and 0.2 wt.%  $\text{C}_{60}$ . The  $\text{C}_{60}$  was added to ensure efficient charge generation at the wavelength of operation. The concentration of EPNA in the films was less than that of FDEAMNST, because at higher loadings of EPNA the films obtained were no longer completely transparent. The solutions were filtered through a 0.2  $\mu\text{m}$  filter and the solvent was allowed to evaporate. Subsequently, the solid film obtained was reduced to powder and stored overnight in a vacuum chamber to ensure maximum solvent removal. The resulting powder was pressed in a stainless steel mould at elevated temperatures. After cooling down, the resulting pellets were sandwiched between two ITO-covered glass plates by applying gentle pressure at 100  $^\circ\text{C}$ . The thickness was fixed by Teflon spacers.

## 5.3. Results and discussion

### 5.3.1. Optical absorption

An important feature of a photorefractive polymer is its absorption spectrum, since this determines the wavelength region in which the polymer can be used. From the results obtained in chapter three, section 3.4.1, it is clear that in the wavelength region of interest the NLO molecule should not absorb, as this can give rise to competing, non-photorefractive gratings. Therefore, to determine at which wavelength the polymer composites can be used, the absorption spectra of the films have been measured (figure 5.2, the inset shows the absorption spectrum in chloroform solution).

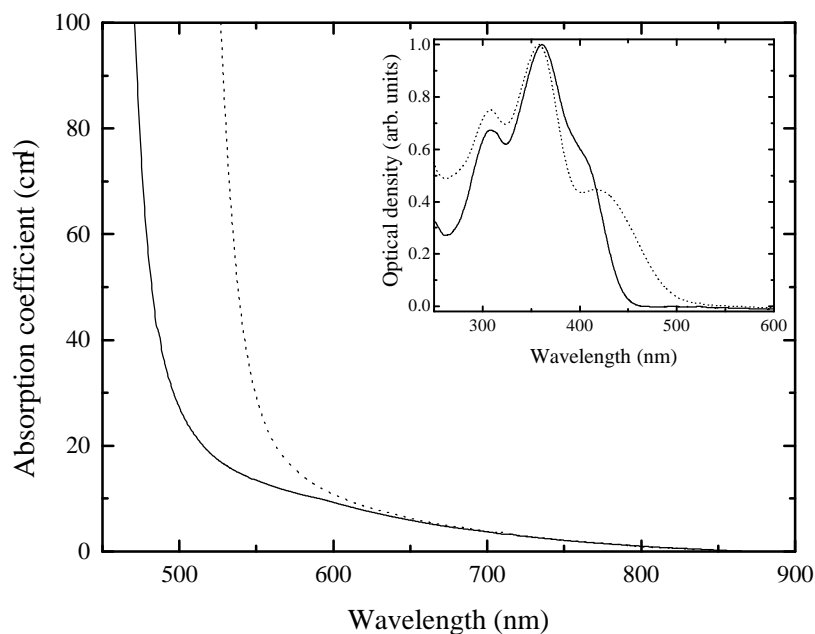


*Fig. 5.2: The absorption spectra of the polyTPD films incorporating EPNA (solid line) and FDEAMNST (dotted line). The inset shows the absorption spectra of polyTPD:EPNA (solid line) and polyTPD:FDEAMNST (dotted line) in chloroform solution.*

The absorption coefficient above 600 nm is very low and is most likely not resulting from absorptions by either EPNA or FDEAMNST. Therefore, the electro-optic and photorefractive characterizations can safely be performed using a He-Ne laser which emits at 633 nm. The absorption coefficients at 633 nm of polyTPD:FDEAMNST:C<sub>60</sub> and polyTPD:EPNA:C<sub>60</sub> are approximately 7 and 8 cm<sup>-1</sup>, respectively.

### 5.3.2 Photorefractive characterization

The intensity of the photorefractive effect depends not only on the strength of the space-charge field but also on the magnitude of the electro-optic effect. The main reason to use a host-guest TPD-based photorefractive polymer instead of the photorefractive polymer described in chapter four, which was based on a bifunctional molecule, is the desire to increase the electro-optic effect. In figure 5.3 the electro-optic coefficients of the polyTPD-based polymers containing EPNA and FDEAMNST are depicted.

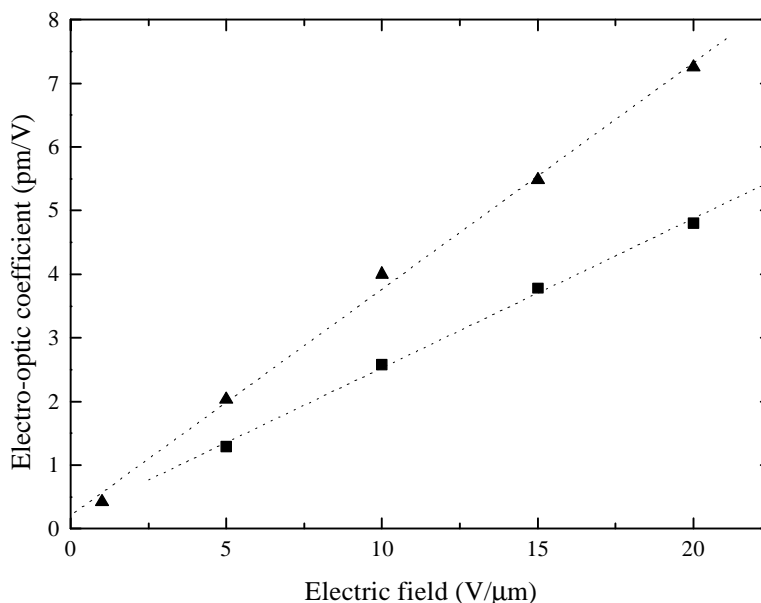


**Fig. 5.3:** The electro-optic coefficients of polyTPD:EPNA (squares) and of polyTPD:FDEAMNST (triangles), measured at a modulation frequency of 1 kHz. The lines are linear fits with exponents 0.36 and 0.23 for the composites containing FDEAMNST and EPNA, respectively.

A linear increase of the electro-optic coefficient with applied electric field is observed for both polymers as a result of the increase in alignment of the NLO molecules. A maximum value of 4.8 pm/V is observed for the EPNA-containing polymer and 7.2 pm/V for the FDEAMNST-containing polymer, both at external electric fields of 20 V/μm. Especially the electro-optic coefficient for the FDEAMNST polymer is large, even in comparison with the highest values obtained for PVK-based photorefractive composites. These large values are the result of the low intrinsic  $T_g$  of polyTPD together with a high degree of loading of the electro-optic molecules. The higher value of the electro-optic coefficient for the FDEAMNST-containing polymer with respect to the EPNA-containing polymer can be explained by the fact that FDEAMNST has a larger hyperpolarizability than EPNA. Furthermore, the concentration of FDEAMNST in the polymer is higher than that of EPNA, which directly increases the electro-optic effect as it is proportional to the amount of electro-optic molecules, and indirectly because it causes a higher orientational freedom due to the increased plasticization. Relative to the electro-optic coefficient of the bifunctional molecule based polymer described in chapter four (1.5 pm/V, at 1 kHz and 10 V/μm), the electro-optic

coefficient has almost doubled for the EPNA-containing polymer, and almost tripled for the FDEAMNST-containing polymer.

To establish whether the polyTPD-based polymers are indeed photorefractive, two-beam coupling experiments were performed.

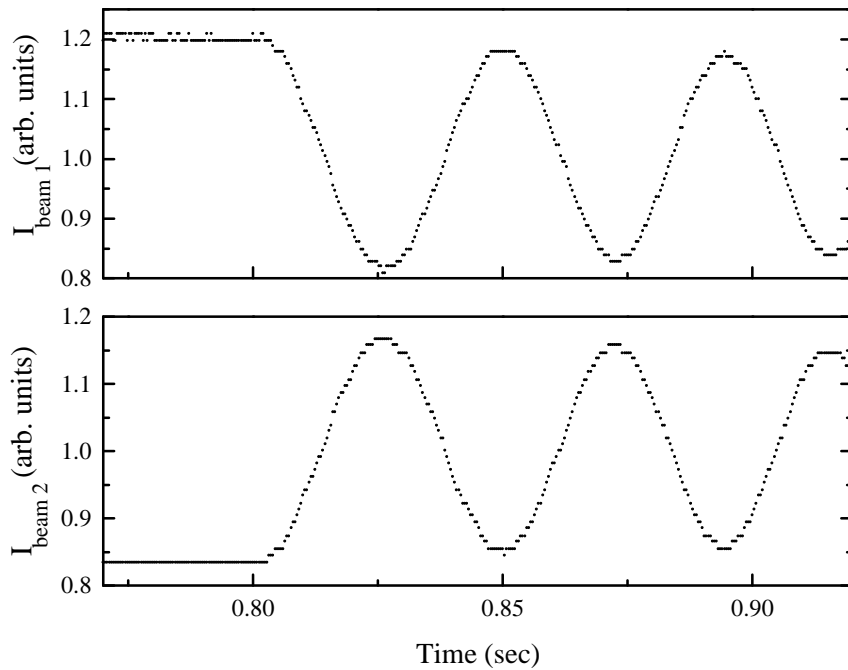


**Fig. 5.4:** Time dependence of the transmitted power of two writing beams in a two-beam coupling experiment for the polyTPD:EPNA:C<sub>60</sub> composite at an applied electric field of 54 V/mm.

Figure 5.4 shows the evolution of the transmitted power of the two writing beams in a two-beam coupling experiment during the translation of the polymer composite employing EPNA as the electro-optic molecule. From the onset of the intensity modulation, a phase shift of 90° between the refractive index grating and the illumination pattern is deduced. This, together with the fact that the two intensities are 180° out of phase, provides evidence for the photorefractive nature of the created grating<sup>8</sup>. The same experiment was done for the sample employing FDEAMNST as the electro-optic molecule (figure 5.5).

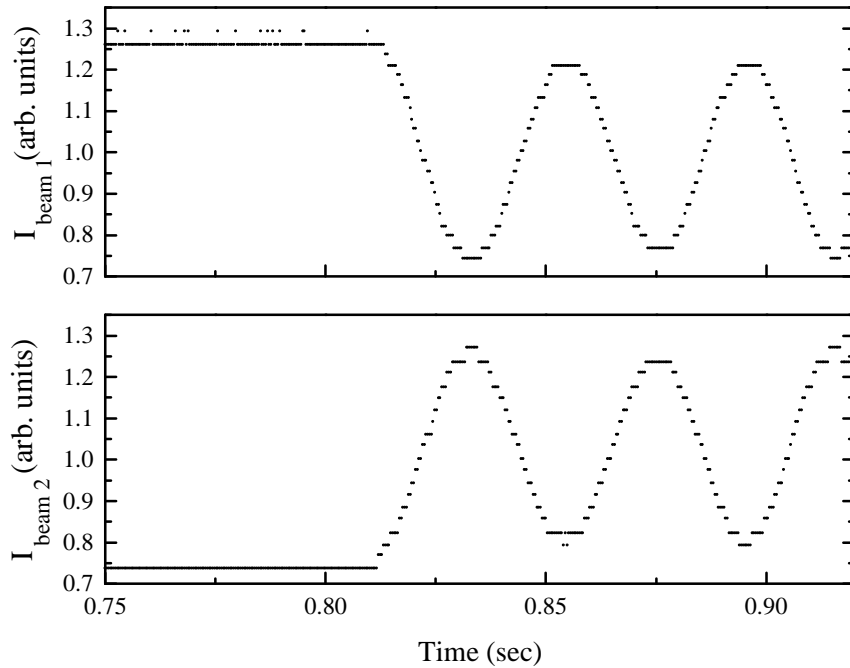


**Fig. 5.5:** Time dependence of the transmitted power of two writing beams in a two-beam coupling experiment for the polyTPD:FDEAMNST:C<sub>60</sub> composite at an applied electric field of 54 V/μm.

In figure 5.5, the intensities of the two beams during the translation of the FDEAMNST-containing composite is shown. At time approximately equal to 0.81 seconds, sample translation begins and the signals on the two photodiodes are modulated as the two beams read out the grating. The two signals are 180° out of phase, indicating the dominance of the refractive index grating. From the onset of the modulation, a phase shift of approximately 90° is deduced.

The amplitude of the light intensity modulation of the two different polyTPD-based composites differs by a factor 1.6. This is most likely caused by the difference in electro-optic effect (a factor 1.5) and not by a change in the magnitude of the space-charge field, for reasons to be discussed below.

In figure 5.6 the gain coefficients for the polyTPD composites containing EPNA and FDEAMNST as a function of applied electric field are depicted.

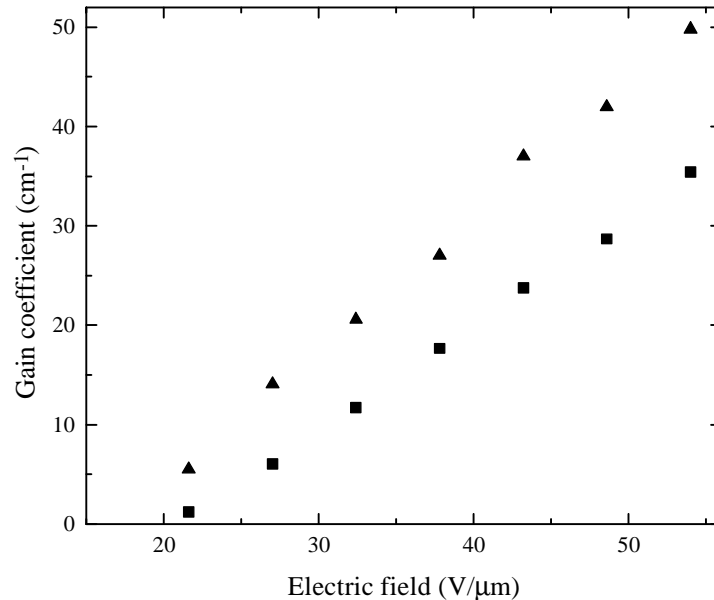


**Fig. 5.6:** The gain coefficient as a function of electric field for the samples polyTPD:EPNA:C<sub>60</sub> (squares) and polyTPD:FDEAMNST:C<sub>60</sub> (triangles).

The maximum values of the gain coefficient are approximately 36 and 49 cm<sup>-1</sup> for the polymers containing EPNA and FDEAMNST, respectively, at an external electric field of 50 V/μm. These values are rather low, especially in view of the high electro-optic coefficients. The gain coefficients increase linearly with electric field at electric fields above 30 V/μm. This is in agreement with the observation of a 90° phase shift between the illumination pattern and the refractive index grating for both composites. According to the standard model, such a phase shift implies a low value for the saturation field as a result of the low trap density<sup>9</sup>. The low concentration of trapping sites is probably caused by the use of the TPD-based charge transport molecule<sup>10</sup>. This means that the space-charge field reaches its maximum value already at low electric fields. Therefore, only at low fields do both the space-charge field and the electro-optic coefficient increase, resulting in the nonlinear behaviour of the gain coefficient. At higher fields, the increase in the gain coefficient is solely due to an increase in electro-optic effect, which results in the observed linear increase. Even though this linear behaviour is in agreement with the standard model, fitting of the curves using the equation derived from the standard model resulted in unrealistic values for the diffusion and saturation fields. This means that the standard model can qualitatively describe the obtained dependence of the gain coefficient on electric field, but not quantitatively.

The dependence of the diffraction efficiencies of the polyTPD composites containing EPNA and FDEAMNST are depicted in figure 5.7.

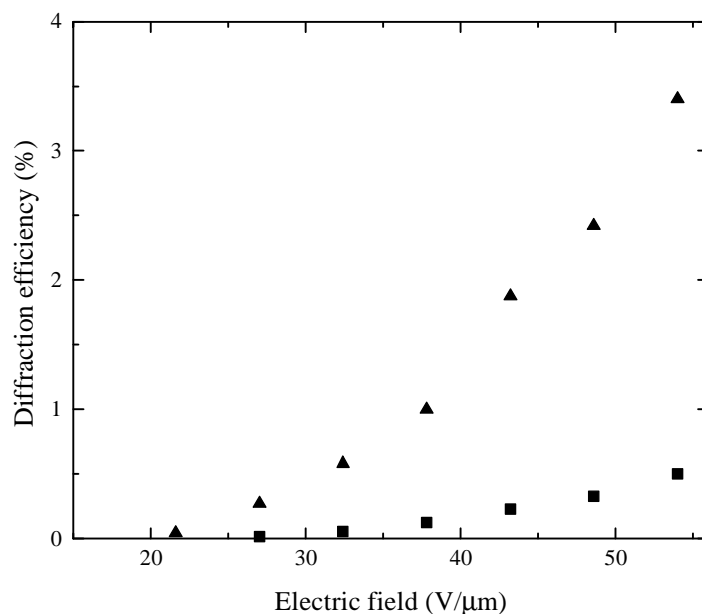


**Fig. 5.7:** The diffraction efficiency as a function of electric field for the samples, polyTPD:EPNA:C<sub>60</sub> (squares) and polyTPD:FDEAMNST:C<sub>60</sub> (triangles).

The diffraction efficiencies of 0.5 and 3.4 % for the polyTPD composite containing EPNA and FDEAMNST, respectively, are again rather small with respect to their electro-optic coefficients. Even though the observed superlinear dependence of the diffraction efficiency with applied electric field, at fields above the saturation field, is predicted by the standard model for materials with small space-charge fields, it was not possible to quantitatively describe the behaviour of the composites using this model.

From the magnitudes of the gain coefficient and diffraction efficiency and their dependence upon electric field it is obvious that the space-charge field is small. Hence, to increase the photorefractive performance it is necessary to increase the space-charge field. In chapter four we were able to increase the space-charge field of the bifunctional molecule based photorefractive polymer by introducing additional trapping sites. We have tried this approach again for the polyTPD-based photorefractive polymers, both by adding DEH and by adding TMPD. In this case, however, no measurable increase in gain coefficient or diffraction efficiency could be observed. This indicates that for polyTPD neither DEH nor TMPD are capable of acting as a trap. The reason for this might be that the difference in HOMO energy levels between polyTPD and DEH or

TMPD is not large enough. Since the HOMO energy level of polyTPD cannot be determined, it was assumed to be approximately equal to that of the basic unit of the polymer, dimethoxy-TPD (MTPD). In chapter two, the energies of the HOMO's of MTPD, MDCTPD (the bifunctional molecule used in chapter four), DEH and TMPD are presented. The energy difference between the HOMO's of DEH or TMPD and that of MTPD has almost become negligible (0.05 eV), whereas the difference was approximately 0.3 eV in the case of MDCTPD. The results obtained in chapter four have shown that the energy difference between the HOMO's measured in the gas phase is not always indicative of the nature of the charge transport in polymers. This was concluded from data concerning oxidation potentials obtained from cyclic voltammetry. These revealed a significant difference in oxidation potentials between DEH and TMPD whereas no such difference in ionization energies obtained from gas phase measurements was observed. For this reason also the cyclic voltammogram of MTPD was measured and an oxidation potential of 0.56 V was found. This value is shifted by 0.21 V towards the oxidation potential of DEH and TMPD (0.44 and 0.09 V respectively). This is in agreement with the decrease in ionization energy difference between the trapping and the transport molecules. Apparently the difference in ionization and oxidation potential between TMPD and MTPD is too small for TMPD to be able to act as a trapping site in this material.

### 5.3.3. Temporal behaviour

The response time of a photorefractive polymer depends on the efficiency of charge generation, the mobility of the created charges and the orientational mobility of the NLO chromophores under the influence of the space-charge field. The decay of the diffraction efficiency of the composite polyTPD:EPNA:C<sub>60</sub> was measured after turning of one of the two writing beams, and the typical decay time was found to be of the order of half a second (figure 5.8). This value is approximately the same as the one that can be deduced from the rise time observed in the gain experiment.

From figure 5.8 it appears that after an initial decay the diffraction efficiency increases again. Such an increase is not expected in the case of only one photorefractive grating. A similar behaviour of the diffraction efficiency decay has been observed before in a photorefractive polymer<sup>11</sup>. In that material the increase of the diffraction efficiency was referred to as revelation. Revelation can only occur if there are different kinds of free carriers. In that case the space-charge field is created first by the most mobile charges but is slowly countercharged with the less mobile charge, decreasing the actual space-charge field and consequently the photorefractive response. Upon uniform illumination the fastest charges will migrate throughout the material first, leaving the less mobile charges behind, which will result in an increase in the space-charge field and hence in diffraction efficiency. Only when these less mobile charges are migrating,

the space-charge field and diffraction efficiency decrease again. From the magnitude of the revelation an indication about the amount of competing charges can be obtained.

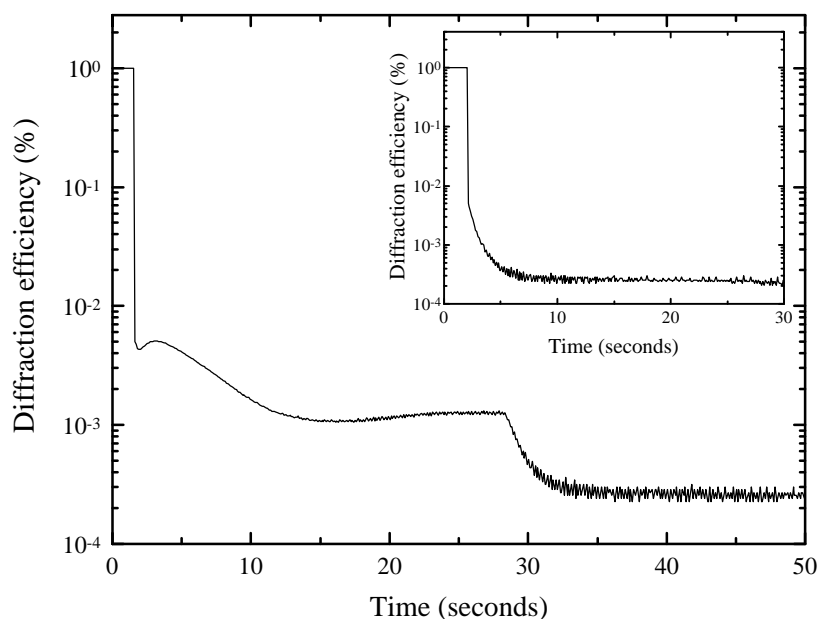


**Fig. 5.8:** The decay of the diffraction efficiency of the composite polyTPD:EPNA:C<sub>60</sub> as a function of time. The large drop in diffraction efficiency observed at approximately 30 seconds is caused by the removal of the electric field. The inset shows the decay of the diffraction efficiency as a function of time for a different sample of the same composition. Both decays were measured under an applied electric field of 50 V/mm.

From figure 5.8 an increase in the diffraction efficiency can be observed. This means that the space-charge field created by the fastest charges (holes) is diminished. Such a decrease in the space-charge field has a dramatic effect on the photorefractive performance and might explain partly the low values obtained for the gain coefficient and diffraction efficiency despite the high electro-optic coefficient. In the case of the inorganic crystal Bi<sub>12</sub>SiO<sub>20</sub>, charges of opposite sign were purposely introduced to verify the existence of revelation<sup>12</sup>. In the photorefractive polymer mentioned, negative charges were found to be present, but the origin was not determined. In our composite the origin of the negative charges is equally unclear; it seems likely that it has to do with the sample preparation procedure. One explanation for the charges could be the presence of negative ions in the solvent used to prepare the composite. It is very

difficult to identify the source of such ions as the concentration necessary to form a competing grating is extremely low (approximately  $10^{16}$  particles per  $\text{cm}^3$ ). The revelation is, however, not always observed. An example of a such a revelation-free diffraction efficiency decay is depicted in the inset of figure 5.8. Here a single exponential decay is obtained for the sample polyTPD:EPNA:C<sub>60</sub>, as is predicted by the standard model. Apparently, depending on unknown and therefore uncontrollable experimental parameters, sometimes revelation is present and sometimes not. The occasional presence of revelation has a large effect on the reproducibility of the experiments from sample to sample. The dependence of the photorefractive parameters upon electric field does not change qualitatively but the magnitude does vary almost by a factor two. As the presence of revelation indicates a decrease of effective space-charge field, the values obtained without (or almost without) revelation were regarded as the material values.

#### 5.4. Conclusion

We have successfully prepared a photorefractive polymer using the charge transport molecule TPD. This was achieved by functionalizing this molecule with two hydroxy groups so that it could be reacted with a dichloroalkane yielding a polyether. From the various dichloroalkanes that were investigated only the use of di-(2-chloroethyl)-hexylamine resulted in a polymer that gave transparent films. In this polymer it was possible to incorporate high amounts of the electro-optic molecules, EPNA and FDEAMNST, which made it electro-optically active. The difference in electro-optic coefficient between the polymers containing EPNA and those containing FDEAMNST is the result of a higher concentration of FDEAMNST. The value of the electro-optic effect for the FDEAMNST-containing polymer is rather large compared to that of other photorefractive polymers. This is attributed mainly to the efficient plasticization by the FDEAMNST molecule resulting in a  $T_g$  of the composite which is very close to room temperature.

The photorefractive nature of the gratings was proven by the existence of a  $90^\circ$  phase shift between the refractive index grating and the illumination pattern. The magnitude of the photorefractive effect expressed by the gain coefficient and the diffraction efficiency was rather small, especially in view of the high electro-optic coefficient. This was attributed to a low value for the space-charge field. Attempts to increase the space-charge field by incorporating additional trapping sites were not successful, probably because of the decreased energy difference between the HOMO of the transport species and that of the trapping molecule. Investigation of the temporal behaviour revealed the existence of a second photorefractive grating originating from negative charges. This second grating has a negative influence on the magnitude of the photorefractive performance and the reproducibility. The origin of these negative

mobile charges is unresolved. As they are not always present, it seems likely that they are introduced during sample preparation procedures.

### 5.5. Experimental Section

Nuclear magnetic resonance (NMR) spectra were taken with a Varian VXR 300 spectrometer. The UV-Vis absorption spectra were recorded using a SLM Aminco 3000 spectrophotometer. The glass transition temperatures ( $T_g$ ) were determined with a Perkin-Elmer DSC-7 series differential scanning calorimeter at a heating rate of 10 °C/min. Molecular weights were determined using a high pressure liquid gel permeation chromatograph coupled with a multiangle laser light scattering (DAWN-DSP, Wyatt techn. Corp.), a refractive index (SHODEX RI-71) and a viscometer detector (Viscotek H502).

All reactions were performed under a dry nitrogen atmosphere. DMF was distilled over  $\text{LiAlH}_4$ , dichloromethane was distilled from  $\text{CaH}_2$  and pentane was distilled from  $\text{P}_2\text{O}_5$ . All chemicals were obtained from either Acros Chimica or Aldrich.

*N,N'*-bis(4-methoxyphenyl)-*N,N'*-diphenyl-[1,1'-biphenyl]-4,4'-diamine **2** A solution of 10 g (0.030 mol) *N,N'*-diphenyl-[1,1'-biphenyl]-4,4'-diamine, 20.9 g (0.090 mol) 4-iodoanisole, 16.56 g (0.120 mol) potassium carbonate and 8.8 g copper bronze in 40 ml hexadecane was stirred under argon atmosphere at 210 °C for three days. After cooling down, the excess iodoanisole was removed together with the solvent by distillation under reduced pressure. The product was extracted by refluxing in 400 ml octane and subsequent hot filtration to remove the inorganic salts. The orange filtrate was purified by column chromatography using silica gel and dichloromethane:pentane (1:1) as the eluent. Evaporation of the solvent yielded 11.6 g (70%) of a white solid.  $^1\text{H}$  NMR ( $\text{CDCl}_3$ )  $\delta$  4.06 (s, 6H), 7.11 (dd, 4H), 7.31-7.51 (m, 18H), 7.66 (dd, 4H).  $^{13}\text{C}$  NMR ( $\text{CDCl}_3$ )  $\delta$  55.68 ( $\text{CH}_3\text{O}$ ), 115.01, 122.16, 123.08, 123.25, 127.31, 127.52, 129.30 (CH-aromatic), 134.28, 140.89, 147.18, 148.28, 156.44 (C-aromatic). Mass (m/e) 587 ( $\text{M}^+$ ), 293.62 ( $\text{M}^{2+}$ ), theoretical mass: 587.257, found: 587.257.

*N,N'*-bis(4-hydroxyphenyl)-*N,N'*-diphenyl-[1,1'-biphenyl]-4,4'-diamine **3** A solution of 10 g (0.018 mol) *N,N'*-bis(4-methoxyphenyl)-*N,N'*-diphenyl-[1,1'-biphenyl]-4,4'-diamine and 8.1 g (0.054 mol) sodium iodide in 100 ml sulpholane is heated to approximately 140 °C until the majority of the starting compounds is dissolved. After cooling down to 60 °C, 6.1 g (0.054 mol) chlorotrimethylsilane was added. The resulting mixture was refluxed for an additional six hours, before cooling down and pouring into a large excess of water. The very viscous precipitate was isolated by careful decantation of the water layer, and subsequently dissolved in methanol. After extracting twice with hexane the methanol was evaporated, and the residue dissolved in

acetone. The solution was slowly added to a large excess of water, after which the crude product solidified. This crude product was filtrated, dried and subsequently purified by column chromatography over silica gel using a mixture of ethyl acetate:dichloromethane (1:20) as the eluent. Evaporation of the solvent yielded 6.75 g (72 %) of the pure product.  $^1\text{H}$  NMR (DMSO- $d_6$ )  $\delta$  6.72 (dd, 4H), 6.83-7.28 (m, 18H), 7.45 (dd, 4H).  $^{13}\text{C}$  NMR (DMSO- $d_6$ )  $\delta$  116.38, 121.72, 121.80, 122.17, 126.72, 127.92, 129.18 (CH-aromatic), 132.66, 138.01, 146.54, 147.53, 154.56 (C-aromatic). Mass (m/e) 520 ( $\text{M}^+$ ), 260 ( $\text{M}^{2+}$ ), theoretical mass: 520.215, found: 520.215.

*Bis(2-hydroxyethyl)hexylamine* A solution of 10 g (0.095 mol) diethanolamine and 7.76 g (0.047 mol) 1-bromohexane in 40 ml isoamyl alcohol was refluxed overnight. The solvent was removed under reduced pressure and the residue was mixed with water and extracted three times with diethyl ether. The combined ether layer was washed with water (three times) and subsequently with diluted hydrochloric acid (three times). The combined hydrochloric acid layer was made basic by adding a solution of 30% NaOH in water. The oily product which was formed was extracted with ether from this basic water solution. After drying the ether layer over  $\text{MgSO}_4$  and evaporating the solvent, 4.2 g (47%) of a pure oil was obtained.  $^1\text{H}$  NMR ( $\text{CDCl}_3$ )  $\delta$  0.88 (m, 3H), 1.27 (m, 6H), 1.44 (m, 2H), 2.36 (s, 2H), 2.52 (t, 2H), 2.67 (t, 4H), 3.61 (t, 4H).  $^{13}\text{C}$  NMR ( $\text{CDCl}_3$ )  $\delta$  13.76 ( $\text{CH}_3$ ), 22.34, 26.48, 26.77, 31.48 ( $\text{CH}_2$ ), 54.55, 55.81 ( $\text{CH}_2\text{N}$ ), 59.33 ( $\text{CH}_2\text{OH}$ ).

*Bis(2-chloroethyl)hexylamine* **4** 5 g (0.026 mol) bis(2-hydroxyethyl)hexylamine was slowly added to 6.9 g (0.058 mol) thionyl chloride, and subsequently refluxed for two hours. After cooling down the resulting mixture was poured into an excess of water, which was subsequently made basic by adding a solution of 10% NaOH in water. The product was extracted with diethyl ether. After drying over  $\text{MgSO}_4$  and evaporation of the solvent, the crude product was obtained. This was purified by distillation under reduced pressure, yielding 3.5 g (0.60%) of a clear liquid which solidified upon standing.  $^1\text{H}$  NMR ( $\text{CDCl}_3$ )  $\delta$  1.02 (t, 3H), 1.41 (m, 6H), 1.56 (m, 2H), 2.67 (t, 2H), 2.99 (t, 4H), 3.63 (t, 4H).  $^{13}\text{C}$  NMR ( $\text{CDCl}_3$ )  $\delta$  13.43 ( $\text{CH}_3$ ), 21.87, 26.12, 26.97, 32.04 ( $\text{CH}_2$ ), 42.02 ( $\text{CH}_2\text{Cl}$ ), 54.24, 56.19 ( $\text{CH}_2\text{N}$ ).

*2-Fluoro-N,N-diethylaniline* **5** A mixture of 22.2 g (0.200 mol) 2-fluoroaniline and 24.3 g (0.133 mol) triethyl phosphate was stirred for 5 hours at 200 °C. The mixture was cooled to 50 °C and a solution of 25 g NaOH in 100 ml water was added followed by refluxing the solution for one hour. Upon cooling the sodium phosphate crystallizes. The oily layer was decanted, diluted with ether and dried over  $\text{MgSO}_4$ . After filtration and evaporation of the solvent the residue was stirred overnight in acetic anhydride. 20 ml of concentrated hydrochloric acid in 30 ml water was added and the clear solution

was washed three times with diethyl ether. The water layer was made basic by adding a 25% NaOH solution in water and the product was collected by extracting the water layer three times with diethyl ether. After drying over MgSO<sub>4</sub>, filtration and evaporation of the solvent, 10.3 g (31%) of a colourless oil was obtained. <sup>1</sup>H NMR (CDCl<sub>3</sub>) δ 1.10 (t, 6H), 3.24 (q, 4H), 6.84 (dd, 2H), 7.24 (dd, 2H).

*3-Fluoro-4-(N,N-diethylamino)benzaldehyde* 18.85 g (0.123 mol) POCl<sub>3</sub> was slowly added to a stirred solution of 5.33 g (0.032 mol) 2-fluoro-*N,N*-diethylaniline and 8.95 g (0.123 mol) dimethylformamide in 30 ml 1,2-dichloroethane. Subsequently the solution was refluxed for two hours, cooled, and poured into water. The resulting mixture was extracted with dichloromethane (three times). After drying over MgSO<sub>4</sub> the solvent together with the 1,2-dichloroethane and the DMF were removed by evaporation under reduced pressure. This crude product was purified by column chromatography over silica gel using ether:hexane (1:2) as the eluent, yielding 3.1 g (50%) of a yellow oil. <sup>1</sup>H NMR (CDCl<sub>3</sub>) δ 1.21 (t, 6H), 3.42 (q, 4H), 6.82 (m, 1H), 7.41-7.53 (m, aromatic, 2H), 9.72 (s, 1H).

*3-Fluoro-4-(N,N-diethylamino)-(E)-b-methyl-(Z)-b-nitrostyrene 6* A mixture of 1.5 g (7.7 mmol) 3-fluoro-4-(*N,N*-diethylamino)benzaldehyde, 0.85 g (11.3 mmol) nitroethane, 0.40 g (5.8 mmol) ammonium acetate and 4.22 g glacial acetic acid was stirred at 80 °C for three hours. After cooling down the solution was poured into water and extracted three times with dichloromethane. The combined dichloromethane layers were washed three times with water and dried over MgSO<sub>4</sub>. After filtration and evaporation of the solvent the crude product was purified by column chromatography over silica gel using dichloromethane:pentane (3:1) as the eluent, yielding 0.90 g (57%) of the pure orange oil. <sup>1</sup>H NMR (CDCl<sub>3</sub>) δ 1.18 (t, 6H), 2.49 (d, 3H), 3.35 (q, 4H), 6.82 (m, 1H), 7.11-7.18 (m, 2H), 8.00 (s, 1H). <sup>13</sup>C NMR (CDCl<sub>3</sub>) δ 12.76 (CH<sub>3</sub>-), 13.94 (CH<sub>3</sub>-), 45.69 (CH<sub>2</sub>-), 117.05, 118.23, 127.91, 133.24 (CH-aromatic), 122.06, 144.15, 144.27 (C-aromatic).

*Polymerization:* A mixture of 3.74 g (7.19 mmol) *N,N'*-bis(4-hydroxyphenyl)-*N,N'*-diphenyl-[1,1-biphenyl]-4,4'-diamine, 1.6 g (7.19 mmol) bis(2-chloroethyl)-hexylamine, 0.82 g (2.4 mmol) of the phase transfer catalyst, tetrabutylammonium hydrogen sulphate (TBAH) and 20 ml chlorobenzene was stirred at 80 °C under argon atmosphere. After 15 minutes 12 ml of a 10 N NaOH-solution was added under vigorous stirring, and the mixture was subsequently stirred for another three hours at 80 °C. After cooling down, the solution was diluted with 50 ml of dichloromethane and washed three times with brine and three times with water. The resulting dichloromethane solution was slowly added to 500 ml of methanol in which the polymer precipitated. The polymer was filtrated and reprecipitated twice from dichloromethane in methanol. Filtration and drying yielded in 4.1 g (86%) of a white polymer.

### 5.6. References

- [1] M. Stolka, J. Yanus, and D.M. Pai, *J. Phys. Chem.* 88, 4707 (1984)
- [2] P. Günter and J.P. Huignard, eds. "*Photorefractive Materials and their Applications I and II*", Topics in Applied Physics vol. 61 and 62, Springer-Verlag (1988)
- [3] P.N. Prasad and D.J. Williams, "*Introduction to Nolinear Optical Effects in Molecules and Polymers*", Wiley Interscience (1991)
- [4] W.E. Moerner and S.M. Silence, *Chem. Rev.* 94, 127 (1994)
- [5] Y. Zhang, R. Burzynski, S. Ghosal and M.K. Casstevens, *Adv.Mater.* 8, 111 (1996)
- [6] S.M. Silence, J.C. Scott, F. Hache, E.J. Ginsburg, P. Jenkner, R.D. Miller, R.J. Twieg and W.E. Moerner, *J. Opt. Soc. Am. B.* 10, 2306 (1993)
- [7] V. Percec, ACS symposium series 326, *Phase-Transfer Catalysis*, chapter 9, C.M. Stark, ed. (1987)
- [8] C.A. Walsh and W.E. Moerner, *J. Opt. Soc. Am. B.* 9, 1642 (1992)
- [9] N.V. Kukhtarev, V.B. Markov, S.G. Odulov, M.S. Soskin and V.L. Vinetskii, *Ferroelectrics* 22, 949 (1979) and *Ferroelectrics* 22, 961 (1979)
- [10] M. Stolka and M.A. Abkowitz, *Synth. Metals* 54, 417 (1993)
- [11] S.M. Silence, C.A. Walsh, J.C. Scott, T.J. Matray, R.J. Twieg, F. Hache, G.C. Bjorklund and W.E. Moerner, *Opt. Lett.* 17, 1107 (1992)
- [12] M.C. Bashaw, T.-P. Ma, R.C. Barker, S. Mroczkowski and R.R. Dube, *Phys. Rev. B.* 42, 5641 (1990)